processes

MDPI

Article

Effect of Acetylation on the Behavior of Hyperbranched Polyglycerols in Supercritical CO_2

Lígia Passos Maia-Obi † and Reinaldo Camino Bazito *

Department of Fundamental Chemistry, Institute of Chemistry, University of São Paulo, Av. Prof. Lineu Prestes, 748, Cidade Universitária, São Paulo 05508-000, SP, Brazil; ligia.maia@ufabc.edu.br

* Correspondence: bazito@iq.usp.br

† Current Address: Engineering, Modeling and Applied Social Sciences Center, Block A, Room 621-1, Federal University of ABC, Avenida Dos Estados, 5001, Santo André 09210-580, SP, Brazil.

Abstract

Processes using CO_2 either as a solvent or as a reactant, for example, in catalyzed chemical reactions, are increasing in interest due to their green characteristics. Hyperbranched polyglycerols have the potential to be used as support for catalysts in these processes, allowing for an efficient separation of the products and the reutilization of the catalyst, but this requires them to absorb CO_2. Acetylating hydroxylated compounds has shown to be an efficient way to increase their CO_2-philicity, and this work aims to understand how acetylation increases the interaction of hyperbranched polyglycerols with different cores with supercritical CO_2. This involves the study of their kinetics of expansion in this media (from 10 to 25 MPa and at 35 °C and 45 °C) and, eventually, their solubility when it happens. The expansion of the acetylated polyglycerols reached up to 66% in volume, while that of non-acetylated ones, in general, do not exceed 10%. Acetylation plays an important role in increasing the expansion of these polymers in the presence of CO_2 and, therefore, in increasing their CO_2-philicity and CO_2 absorption, making them potential materials to be used in biphasic (polymer/CO_2) reaction systems.

Keywords: hyperbranched polyglycerol; supercritical CO_2; acetylation; phase behavior; CO_2 swelling

Academic Editor: Ali Aminian

Received: 26 June 2025
Revised: 18 July 2025
Accepted: 4 August 2025
Published: 8 August 2025

Citation: Maia-Obi, L.P.; Bazito, R.C. Effect of Acetylation on the Behavior of Hyperbranched Polyglycerols in Supercritical CO_2. *Processes* **2025**, *13*, 2510. https://doi.org/10.3390/pr13082510

1. Introduction

Hyperbranched polyglycerols (HPG-OHs) are polyether polyols formed by glycerol residual units organized in an imperfect dendritic structure [1]. They are easier to prepare than dendrimers but keep the same unique properties, when compared with linear analogs, such as the presence of nanocavities and the high concentration of end groups. The first leads to a larger free volume and a good capacity to incorporate solutes [2,3], and the second leads to a core–shell environment, where the end groups work as a shell, which can be further functionalized, considerably changing the properties of the polymer and its range of applications [4].

Acetylation is a chemical modification that has been used to increase the CO_2-philicity of different materials. A good interaction, and therefore, the absorption of CO_2 in a polymer, results in its swelling. Applications that rely on the sorption of CO_2 in a polymer will be more efficient when intense swelling is observed. For instance, reactions that occur in a CO_2 expanded polymeric phase will be faster when a higher concentration of CO_2 is present in this phase. Also, impregnation of active molecules can be achieved as the process involves

an increase in the distance between the polymer chains and lowering their intermolecular interactions, allowing those molecules to be carried by the CO_2 into the polymeric matrix, and to establish intermolecular interactions with the polymer chains so higher loads can be attained. Processes where CO_2 is used as a plasticizer to decrease the melting point and the glass transition temperature of the polymer, such as extrusion, blending, obtention of composites, or foaming, will also benefit from it making them feasible and suitable at lower CO_2 pressures.

The swelling of a polymer by CO_2 is related to specific intermolecular interactions between the polymer and the CO_2, to the polymer chain flexibility, free volume, and weak polymer–polymer and solvent–solvent intermolecular interactions, leading to an increase in both the solubility of CO_2 into the polymer phase and the solubility of the polymer into the CO_2 phase [5,6]. The acetylation functionalizes hydroxyl or analog groups, removing hydrogen bonds from the material, which reduces the intermolecular interactions between the chains. Moreover, despite CO_2 being an apolar molecule, it presents a charge separation of high amplitude and a significant quadrupolar moment, which allows it to undergo specific Lewis's acid–base interactions with acetyl groups, where the CO_2 oxygen interacts with the α-hydrogen of the acetyl group, and its carbon interacts with the oxygen of the acetyl group, strongly increasing the interaction of the polymer with the fluid [5,6]. Indeed, Nasir and co-workers acetylated various fractions of phospholipids from soybean and found out that the solubility in supercritical CO_2 ($scCO_2$) increased, resulting in a cloud point of 13 MPa at 40 °C for the most soluble fraction [7]. Potluri and co-workers showed the high solubility of acetylated cyclodextrins in $scCO_2$ [8], and Lambert and Ingrosso showed the importance of the acetylation of sugars for their solvation in $scCO_2$ using a molecular dynamics study [9]; Huang and co-workers used peracetylated-β-cyclodextrin as an additive to increase the viscosity of $scCO_2$ [10], and we showed that this solubility allowed for the complexation of Ibuprofen in the same acetylated cyclodextrin [11]. Indeed, in poly (vinyl acetate), the acetyl groups promote its solubility in $scCO_2$ and the solubility of CO_2 into the polymer phase [12–15]; moreover, an increase in the free volume of this polymer by the insertion of branched segments increases its solubility [15].

HPG-OHs possess hydroxyl end groups that can be easily acetylated, generating a CO_2-philic material. Acetylated hyperbranched polyglycerols (HPG-Acs) will have, therefore, the potential for applications such as a matrix for active molecules' impregnation in $scCO_2$ or as a green solvent in CO_2 biphasic reaction systems. Indeed, acetylated polymers have been used as a matrix to impregnate molecules assisted by $scCO_2$. For instance, Valor and co-workers developed a poly (vinyl acetate)/polypyrrole scaffold impregnated with gallic acid for its controlled release using $scCO_2$ [16], and cellulose acetate was used to impregnate menthol and vanillin successfully [17]. Their potential to be used in biphasic systems using CO_2 lays on the fact that those systems have a need for green solvents that can absorb CO_2, solubilize reactants, and support/solubilize/impregnate catalysts. HPG-Acs are non-volatile and non-toxic materials and can act similarly to ionic liquids in those systems but in a much greener way. The solubilization of CO_2 has the potential to decrease their viscosity and enhance the transport properties for a reaction to occur, while favoring the desorption of the products. Indeed, the solubility properties can be tuned by varying the pressure and temperature, and $scCO_2$ can act as a non-reactional phase representing a reservoir for reactants and products enabling an easy reuse of the catalytic/polymer phase [18].

The aim of this study is to understand the impact of the acetylation and polymer structure on the behavior of hyperbranched polyglycerols in supercritical CO_2 through their volumetric expansion. HPG-OHs and HPG-Acs bearing three different cores were chosen in order to provide polymers with slightly different polarities for each class, increasing

from the ones with cores based on the polyols in this sequence: dodecanediol < glycerol < tetraethyleneglycol. Moreover, polymers bearing each core were studied in two different molar masses (Mns) in order to evaluate the impact of the molecular size on the behavior of both HPG-OHs and HPG-Acs in $scCO_2$.

2. Experimental

2.1. Materials

Hyperbranched polyglycerols (HPG-OHs), Figure 1 and Table 1, were previously synthesized via the Ring Opening Polymerization of glycidol [19] using glycerol (GL), dodecanediol (DD), and tetraethyleneglycol (TEG) as initiators, in two different Mns for each initiator. Acetic anhydride (98%, Merck, São Paulo, Brazil) and dichloromethane (Analytical grade, Vetec, São Paulo, Brazil) were distilled prior to use, and pyridine (98%, Vetec, São Paulo, Brazil) was distilled prior to use and kept over molecular sieves (3 Å, Sigma-Aldrich, Cotia, Brazil). Dimethylaminopyridine (DMAP, 99%, Sigma-Aldrich, Cotia, Brazil) and liquid CO_2 (99.98%, Oxilumen, São Paulo, Brazil) were used as received.

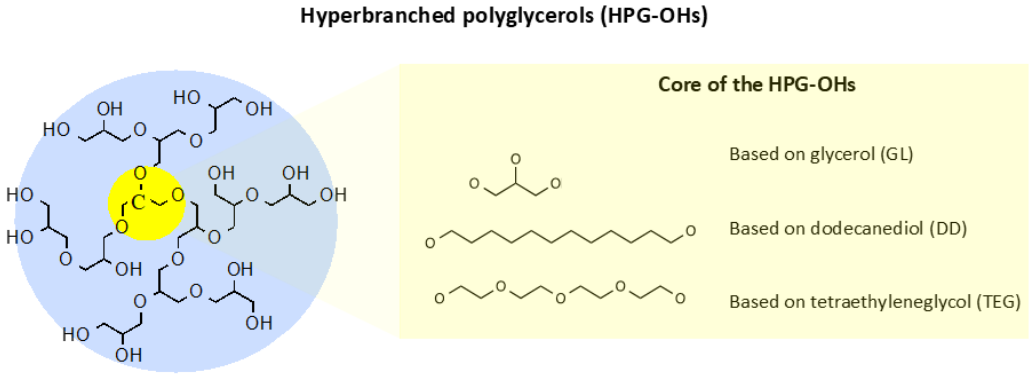

Figure 1. Representation of the studied hyperbranched polyglycerols.

Table 1. Characteristics of the HPG-OHs.

Code	Initiator	Mn (g mol^{-1})	Đ (Mn/Mw) [a]	DB [b]	nOH [c]
GL-HPG-OH-1	GL	562	1.06	0.41	7.6
GL-HPG-OH-2	GL	932	1.09	0.45	13.5
DD-HPG-OH-1	DD	547	1.06	0.23	6.7
DD-HPG-OH-2	DD	804	1.18	0.36	10.1
TEG-HPG-OH-1	TEG	604	1.08	0.15	7.5
TEG-HPG-OH-2	TEG	855	1.10	0.43	10.9

[a] Polymer Dispersity. [b] Degree of branching [19]. [c] Average number of mols of hydroxyl groups per mol of HPG-OH; the method for calculation is presented in the Supporting Information Section.

2.2. Analytical Methods

Mass spectroscopy with electrospray ionization (ESI-TOF-MS) was carried out in a MicroTOF QII Bruker spectrometer (Billerica, MA, USA) operating with a collision energy of 30 eV, using methanol as solvent, to determine the Mn of the polymers.

Nuclear magnetic resonance (^{1}H and ^{13}C NMR) analysis was carried on a Varian Inova spectrometer operating at 300 MHz for ^{1}H and 75 MHz for ^{13}C. The acetylation degree (%AD) was determined by ^{1}H NMR (in DMSO-d_6), using the relative number of

hydrogens of the peaks at δ = 1.90–2.15 ppm (C**H**$_3$CO, 3H) and δ = 4.30–4.85 ppm (R-O**H**, 1H), following Equation (1).

$$\% \, AD = \left(\frac{\left(\frac{\int 1.90 \text{ ppm} - 2.15 \text{ ppm}}{3} \right)}{\left(\left(\frac{\int 1.90 \text{ ppm} - 2.15 \text{ ppm}}{3} \right) + \int 4.30 - 4.85 \text{ ppm} \right)} \right) .100\% \quad (1)$$

Thermogravimetry (TG/DTA) was performed on a Shimadzu DTG-60/60H thermogravimetric balance (Shimadzu, Kyoto, Japan) under a N_2 stream with a flow rate of 50 mL min^{-1}, at a scanning rate of 20 °C min^{-1}, and scanning temperatures between room temperature and 800 °C. The thermal decomposition values (T_d) were calculated as the tangent of the first mass loss event. Differential Scanning Calorimetry (DSC) was performed using the Shimadzu DSC-60 calorimeter (Shimadzu, Kyoto, Japan), under a N_2 stream with a flow rate of 100 mL min^{-1}, with a scan rate of 10 °C min^{-1} (16 °C min^{-1} for the HPG-OHs [19]), and scan temperatures between −100 and 150 ° C, whose acquisition was preceded by a cycle of heating from room temperature to 150 °C and cooling from 150 °C to −100 °C at the same speed [19,20].

2.3. General Procedure for the Acetylation of the HPG-OHs

Acetylated hyperbranched polyglycerols (HPG-Acs) were obtained from HPG-OHs using acetic anhydride. A given mass of the HPG-OH, equivalent to 50 mmol of hydroxyl groups, acetic anhydride (6.64 g, 65 mmol), DMAP (0.98 g, 8 mmol), 20 mL of pyridine, and 60 mL of dichloromethane were introduced in a 250 mL round-bottom flask equipped with a magnetic rod. The flask was placed in an oil bath over a stirring heating place. The reaction media was kept under N_2 and refluxed and stirred for 24 h. The dichloromethane was removed by rotative evaporation, and the crude material was dissolved in ethyl acetate. The solution was washed with HCl 1M until the presence of pyridine in the organic phase was not detected by TLC (Thin Layer Chromatography) and subsequently washed with a saturated solution of sodium bicarbonate, then deionized water. The solution was dried over anhydrous magnesium sulfate for 24 h, and the solvent was removed using a rotating evaporator.

GL-HPG-Ac-1: ^{1}H NMR (25 °C in d_6-DMSO, δ in ppm): 5.20–4.85 (m, 3.35 H, -C**H**-OCOCH$_3$), 4.30–3.90 (m, 3.98 H, and -C**H$_2$**-OCOCH$_3$), 3.90–3.10 (m, 63.92 H, and -OC**H$_2$**C**H**(O-)C**H$_2$**O-), and 2.01 (m, 17.07 H, and -OCOC**H$_3$**). ^{13}C NMR (25 °C in CDCl$_3$, δ in ppm): 170.7–170.3 (-**C**OCH)), 78.77 and 77.27 (-**C**HOCH$_2$), 71.1–68.00 (-CH-O**C**H$_2$CH, -CH$_2$-O**C**H$_2$CH, and -**C**HOH), 63.64, 63.3–62.2 (-**C**H$_2$OH), and 21.1–20.6 (-CO**C**H$_3$). ESI-TOF-MS: Mn = 1114 g mol^{-1}; Đ = 1.07. AD = 100%.

GL-HPG-Ac-2: ^{1}H NMR (25 °C in d_6-DMSO, δ in ppm): 5.15–4.85 (m, 0.54 H, -C**H**-OCOCH$_3$), 4.85–4.35 (s broad, 0.05 H, and O**H**), 4.35–3.85 (m, 1.00 H, and -C**H$_2$**-OCOCH$_3$), 3.85–3.10 (m, 6.30 H, and -OC**H$_2$**C**H**(O-)C**H$_2$**O-, H_2O (trace)), and 2.01 (m, 3.00 H, and -OCOC**H$_3$**). ^{13}C NMR (25 °C in CDCl$_3$, δ in ppm): 170.7–170.3 (-**C**OCH)), 78.75 and 77.27 (-**C**HOCH$_2$), 71.4–68.00 (-CH-O**C**H$_2$CH, -CH$_2$-O**C**H$_2$CH, and -**C**HOH), 63.60 and 62.3 (-**C**H$_2$OH), and 21.1–20.6 (-CO**C**H$_3$). ESI-TOF-MS: Mn = 1499 g mol^{-1}; Đ = 1.03. AD = 95%.

DD-HPG-Ac-1: ^{1}H NMR (25 °C in d_6-DMSO, δ in ppm): 5.15–4.90 (m, 0.65 H, and -C**H**-OCOCH$_3$), 4.90–4.35 (s broad, 0.01 H, and O**H**), 4.30–3.85 (m, 4.10 H, and -C**H$_2$**-OCOCH$_3$), 3.85–3.10 (m, 27.61 H, -OC**H$_2$**C**H**(O-)C**H$_2$**O-, -CH$_2$C**H$_2$**O-, and H_2O (trace)), 2.10–1.95 (m, 7.86 H, and -OCOC**H$_3$**), and 1.7–1.15 (m, 20.0 H, and -CH$_2$C**H$_2$**CH$_2$-). ^{13}C NMR (25 °C in CDCl$_3$, δ in ppm): 171.3–170.3 (-**C**OCH)), 71.8–68.00 (-CH-O**C**H$_2$CH, -CH$_2$-O**C**H$_2$CH, and -**C**HOH), 64.65 (-**C**H$_2$CH$_2$O- and -CH$_2$**C**H$_2$O-), 62.98 (-**C**H$_2$OH), 29.55–25.80 (-CH$_2$C**H$_2$**CH$_2$-), and 21.1–20.6 (-CO**C**H$_3$). ESI-TOF-MS: Mn = 1102 g mol^{-1}; Đ = 1.08. AD = 100%.

DD-HPG-Ac-2: ^{1}H NMR (25 °C in d_6-DMSO, δ in ppm): 5.30–4.80 (m, 5.99 H, and -C**H**-OCOCH$_3$), 4.80–4.40 (s broad, 0.02 H, and O**H**), 4.35–3.90 (m, 10.77 H, and -C**H$_2$**-OCOCH$_3$), 3.80–3.15 (m, 71.84 H, -OC**H$_2$**C**H**(O-)C**H$_2$**O-, -CH$_2$C**H$_2$**O-, and H$_2$O (trace)), 2.05–1.95 (m, 31.96 H, and -OCOC**H$_3$**), and 1.65–1.05 (m, 20.0 H, and -CH$_2$C**H$_2$**CH$_2$-). ^{13}C NMR (25 °C in CDCl$_3$, δ in ppm): 170.5–170.3 (-**C**OCH)), 78.84 (-**C**HOCH$_2$), 71.8–68.00 (-CH-O**C**H$_2$CH, -CH$_2$-O**C**H$_2$CH, and -**C**HOH), 64.54 (-**C**H$_2$CH$_2$O- and -CH$_2$**C**H$_2$O-), 62.59 (-**C**H$_2$OH), 29.55–25.80 (-CH$_2$C**H$_2$**CH$_2$-), and 21.3–20.3 (-CO**C**H$_3$). ESI-TOF-MS: Mn = 1392 g mol^{-1}; Đ = 1.04. AD = 100%.

TEG-HPG-Ac-1: ^{1}H NMR (25 °C in d_6-DMSO, δ in ppm): 5.20–4.88 (m, 0.52 H, and -C**H**-OCOCH$_3$), 4.88–4.55 (s broad, 0.03 H, and O**H**), 4.40–3.88 (m, 1.08 H, and -C**H$_2$**-OCOCH$_3$), 3.88–3.05 (m, 4.70 H, -OC**H$_2$**C**H**(O-)C**H$_2$**O-, -OC**H$_2$**C**H$_2$**O-, and H$_2$O (trace)), and 2.05–1.95 (m, 3.00 H, and -OCOC**H$_3$**). ^{13}C NMR (25 °C in CDCl$_3$, δ in ppm): 170.7–170.2 (-**C**OCH)), 77.27 (-**C**HOCH$_2$), 71.0–68.00 (-CH-O**C**H$_2$CH, -CH$_2$-O**C**H$_2$CH, -**C**HOH, and -OC**H$_2$**C**H$_2$**O-), 63.60 and 62.3 (-**C**H$_2$OH), and 21.1–20.6 (-CO**C**H$_3$). ESI-TOF-MS: Mn = 1337 g mol^{-1}; Đ = 1.04. AD = 97%.

TEG-HPG-Ac-2: ^{1}H NMR (25 °C in d_6-DMSO, δ in ppm): 5.20–4.85 (m, 0.55 H, and -C**H**-OCOCH$_3$), 4.85–4.55 (s broad, 0.03 H, and O**H**), 4.33–3.82 (m, 1.00 H, and -C**H$_2$**-OCOCH$_3$), 3.72–3.35 (m, 4.70 H, -OC**H$_2$**C**H**(O-)C**H$_2$**O-, and -OC**H$_2$**C**H$_2$**O-), 3.31 (s, 0.95 H, and H$_2$O (trace)), and 2.05–1.95 (m, 3.06 H, and -OCOC**H$_3$**). ^{13}C NMR (25 °C in CDCl$_3$, δ in ppm): 170.7–170.15 (-**C**OCH)), 78.74 and 77.27 (-**C**HOCH$_2$), 71.50–68.00 (-CH-O**C**H$_2$CH, -CH$_2$-O**C**H$_2$CH, -**C**HOH, and -OC**H$_2$**C**H$_2$**O-), 63.56, 62.61, and 62.15 (-**C**H$_2$OH), and 21.0–20.6 (-CO**C**H$_3$). ESI-TOF-MS: Mn = 1301 g mol^{-1}; Đ = 1.04. AD = 97%.

2.4. Behavior in Dense CO_2

The behavior of the polymers in dense CO_2 was assessed by volumetric expansion and cloud point experiments using a phase monitor (Thar Instruments SPM20) equipped with a high-pressure variable-volume (5–15.5 mL) view cell monitored by a CCD camera, a mechanical stirrer, a pressure controller, and heaters (Figure 2). The system was fed with CO_2 using a high-pressure syringe pump (ISCO model 260D series). The determination of the volumetric expansion was performed placing a 1 cm long and 0.52 cm in diameter glass tube containing the material being studied in the field of view of the camera of the phase monitor. The system was heated up to the desired temperature and pressurized with CO_2 to the desired pressure. Images were obtained periodically until the stabilization of the volume of the polymer phase was attained (about 100 min). V_0 (volume of the polymer before CO_2 absorption) was determined obtaining images of the system before the pressurization. These images were treated using the software ImageJ v.1.49m [21], converting the height of the material inside the tube to volume for the calculation of the percentage of variation over time (Equation (2), where V_0^{pol} is the initial volume of the polymer and V^{pol} is the volume of the polymer along time). Figure S1 illustrates the determination of the heights. Calibration curves of the height of the polymer phase in relation to its volume were performed for all the conditions studied. Partial solubility was measured as the percentage of weight loss (%) of the samples (Equation (3), where m_0^{pol} is the initial mass of the polymer and m^{pol} is the final mass of the polymer along time). The conditions studied were {10 MPa, 45 °C, and 0.50 g.mL^{-1}}, {15 MPa, 45 °C, and 0.74 g.mL^{-1}}, and {25 MPa, 35 °C, and 0.90 g.mL^{-1}}. The error in volume measurements lies around 2%.

$$\%s = \frac{\left(V^{pol} - V_0^{pol}\right).100\%}{V_0^{pol}} \quad (2)$$

$$\% \; weight \; loss = \frac{\left(m_0^{pol} - m^{pol}\right).100\%}{m_0^{pol}} \quad (3)$$

DD-HPG-Ac-1 was also studied through the determination of their cloud pressures at concentrations of 0.1 and 0.5%wt., at 25, 35, 45, 55, and 65 °C. The experiments were performed by adding the appropriate amount of polymer and CO_2 to the phase monitor to obtain the aimed concentrations. The temperature was set and stabilized, and the pressure of the system was increased from approximately 7.0 MPa to 30.0 MPa by decreasing its volume. The volume was then slowly increased to decrease the pressure to observe the cloud point pressures visually. This cycle of pressurization and depressurization was performed at least five times.

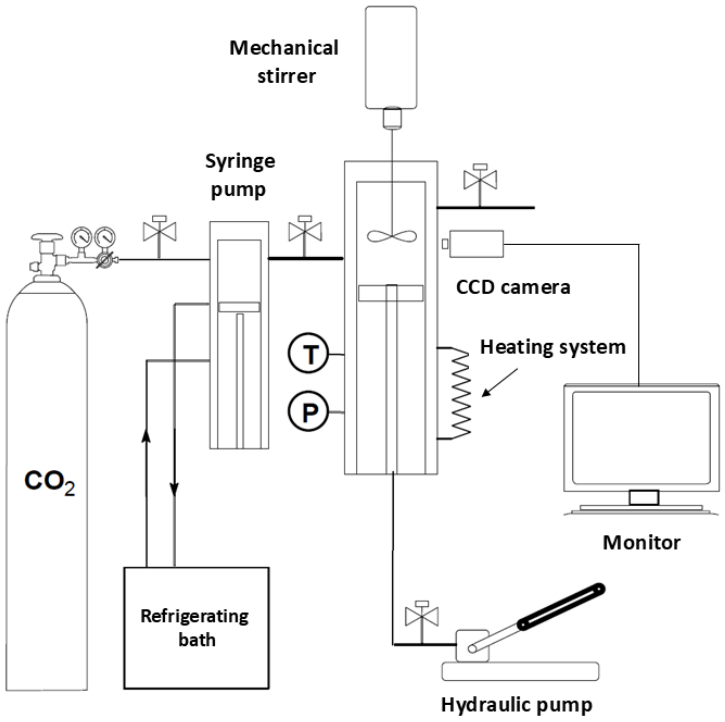

Figure 2. Scheme of the phase monitor.

3. Results and Discussion

3.1. Synthesis of the HPG-Acs

The HPG-Acs were obtained from the HPG-OHs with high purity, as demonstrated by the NMR analyses. The characteristics of the HPG-Acs synthesized are summarized in Table 2. The acetylation degrees (%ADs) were equal or close to 100%. The values are higher for the polymers with lower Mns and lower polarities. Lower molecular masses provide more accessibility to the hydroxyl groups of the HPG-OHs, and lower polarities favor their interaction with the reaction solvent, also helping the accessibility to the hydroxyl groups. Moreover, since the increase in the Mn is given by an increase in the number of glycerol units in the polymer, it also increases the polarity of the HPGs bearing the least polar core, the DD. The Mn of the HPG-Acs increased in relation to their non-acetylated precursors, which can be explained by the addition of the acetyl groups, and also by the loss of the molecules with lower Mns during the purification steps of their syntheses.

Table 2. Characteristics of the HPG-Acs.

Code	Initiator	%AD	Mn (g mol^{-1})	Đ (Mn/Mw) [a]
GL-HPG-Ac-1	GL	100	1114	1.07
GL-HPG-Ac-2	GL	95	1499	1.03
DD-HPG-Ac-1	DD	100	1102	1.08
DD-HPG-Ac-2	DD	100	1392	1.04
TEG-HPG-Ac-1	TEG	97	1337	1.04
TEG-HPG-Ac-2	TEG	97	1301	1.04

[a] Polymer Dispersity.

3.2. Thermal Characterization

The thermal behavior of the studied HPG-OHs and HPG-Acs is presented in Table 3. The HPG-OH samples have a broad range of decomposition temperatures (T_d), from 180 °C to 335 °C. This broad range reflects the increase in the T_d with the increase in the Mn of the polymers bearing the same structure [22]. This increase is not verified by the pair GL-HPG-OH-1 and GL-HPG-OH-2 because, in addition to the difference in Mn, they present differences in their structures. The first possesses a branched cyclic structure while the second one possesses a mix of branched cyclic and non-cyclic structures; those differences are a natural consequence of the reaction mechanism and synthetic methodology. The acetylation of the polymers caused, in general, a decrease in the T_d values due to the introduction of the labile acetyl group into the molecules; however, this is in part balanced by the increase in Mn after acetylation, which contributes to higher T_ds. Despite the lower T_ds for the acetylated polymers, processes involving these polymers can be carried out at temperatures up to 200 °C, an adequate value for a range of applications, including their use as reaction media in the presence of CO_2, whose reactions are normally carried out in low or mild temperatures (35 °C to 60 °C) [23].

Table 3. Thermal behavior of the HPG-OHs and HPG-Acs.

Code	T_d (°C)	T_g1 (°C)	T_g2 (°C)	M_p (°C)
GL-HPG-OH-1	334.2	−48.4, −31.2	-	-
GL-HPG-OH-2	298.3	−53.2	-	-
DD-HPG-OH-1	183.9	−48.9, −35.6	−16.0	49.1
DD-HPG-OH-2	329.1	−48.2, −30.7	−8.9	32.8
TEG-HPG-OH-1	305.8	−45.6, −27.1	-	-
TEG-HPG-OH-2	330.4	−59.4, −47.2	-	-
GL-HPG-Ac-1	240.5	−31.5	-	-
GL-HPG-Ac-2	337.7	−25.9	-	-
DD-HPG-Ac-1	201.0	−55.5	-	−70–33 [a]
DD-HPG-Ac-2	230.1	−46.2	-	-
TEG-HPG-Ac-1	237.9	−41.9	-	-
TEG-HPG-Ac-2	219.0	−31.2	-	-

[a] Several peaks.

The glass transition temperatures (T_gs) of the HPG-OHs were identified in two different regions, the first between −60 °C to −27 °C (T_g1), and the second between −16 °C and −8 °C (T_g2). Most polymers presented more than one T_g at the first region. Goodwin and co-workers demonstrated that this class of polymer can present different T_gs due to the presence of structures with different branching degrees because of their synthetic route, which impacts the mobility of the chains and forms different domains [24]. The T_gs at the first region was verified for all polymers and can be attributed to different structures of the HPG-OH: cyclic and inimeric structures (−60 °C to −50 °C) [20,24,25]; initiator-based

structures (−30 °C to −20 °C), given that high Mn molecules will present an additional lower T_g up to −80 °C, referring to the core structure that differentiates from the more external groups as the Mn increases [20,24,25]; and hydroxyl polar domains (−53 °C to −10 °C) [26]. DD-HPG-OH-1 and DD-HPG-OH-2 are the only ones to present T_g2 and M_ps due to the dodecanediol (DD) chain capacity to generate crystalline regions in the polymers, which does not happen for the other polymers due to the higher degree of branching (DB) of GL, and the flexibility of their core chains, regarding TEG. The T_g2 can be attributed to the glass transition associated with the DD chain and surrounding segments. The acetylation of the HPG-OHs led to single events of T_g1, which is a reflex of the loss of the hydrogen bond at the terminal groups of the polymers. This also causes an increase in polymer mobility, which results in the disappearance of the T_g2 events and of the M_p of the DD-HPG-Ac-2. Moreover, the new values are a result of a balance of the mobility increase (contributing negatively) and of the Mn increase (contributing positively) resulting from the acetylation; moreover, they are also a result of the polarity and DB of the polymers. The polarity of the polymers are as follows: DD-HPG-Ac-1 < DD-HPG-Ac-2 < GL-HPG-Ac-1 < GL-HPG-Ac-2 < TEG-HPG-Ac-1 ≈ TEG-HPG-Ac-2. TEG-HPG-Ac-1 and TEG-HPG-Ac-2, however, do not present the highest T_gs among the samples, due to their lower DBs (DB is lower for the TEG-HPG-Ac-1). The DBs for the polymers DD-HPG-Ac-1 and DD-HPG-Ac-2 are also low, contributing for these polymers to present the lowest T_gs.

3.3. Behavior in Dense CO_2 of the HPG-OHs

The study of the behavior of HPG-OHs was performed in three different CO_2 densities: 0.50 $g.mL^{-1}$ {10 MPa, 45 °C}, 0.74 $g.mL^{-1}$ {15 MPa, 45 °C}, and 0.90 $g.mL^{-1}$ {25 MPa, 35 °C}. This was necessary because preliminary studies showed that volumetric expansion, because of the solubilization of CO_2 in the polymer, increases as a function of the density of CO_2.

The visual observation of the behavior of these polymers, illustrated in Figure 3, shows that upon contact with the $scCO_2$, their viscosity reduces, and bubbling is presented upon decompression (Figure 3a). For polymer DD-HPG-OH-2 (Figure 3b), due to its solid nature at the studied temperatures, a change in viscosity was not observed when the system was pressurized, but cracking is observed upon decompression. These behaviors demonstrate that CO_2 is able to solubilize into these polymer phases.

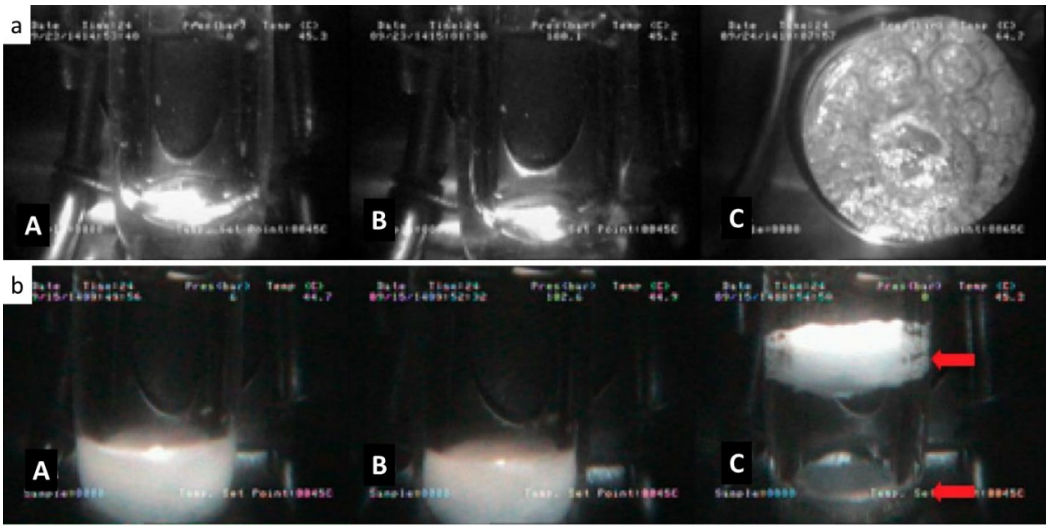

Figure 3. Visualization of the behavior of the polymers (**a**) TEG-HPG-OH-1 and (**b**) DL-HPG-OH-2: (**A**) before pressurization, (**B**) after pressurization, and (**C**) during depressurization. The red arrows point out the two pieces of polymer generated upon depressurization.

The kinetic study of expansion in $scCO_2$ allowed for the verification of the evolution of the expansion percentage of the polymers as a function of time and the maximum expansion attained when the system is in equilibrium. The volume of the polymer phase stabilizes, in general, in less than 20 min, but polymers presenting higher solubilities/expansions required longer times. The graphics presenting the kinetics of expansion are presented in the supporting information.

Figure 4 shows the final expansion, in volume percentage, of the polymers studied as a function of the density of the system.

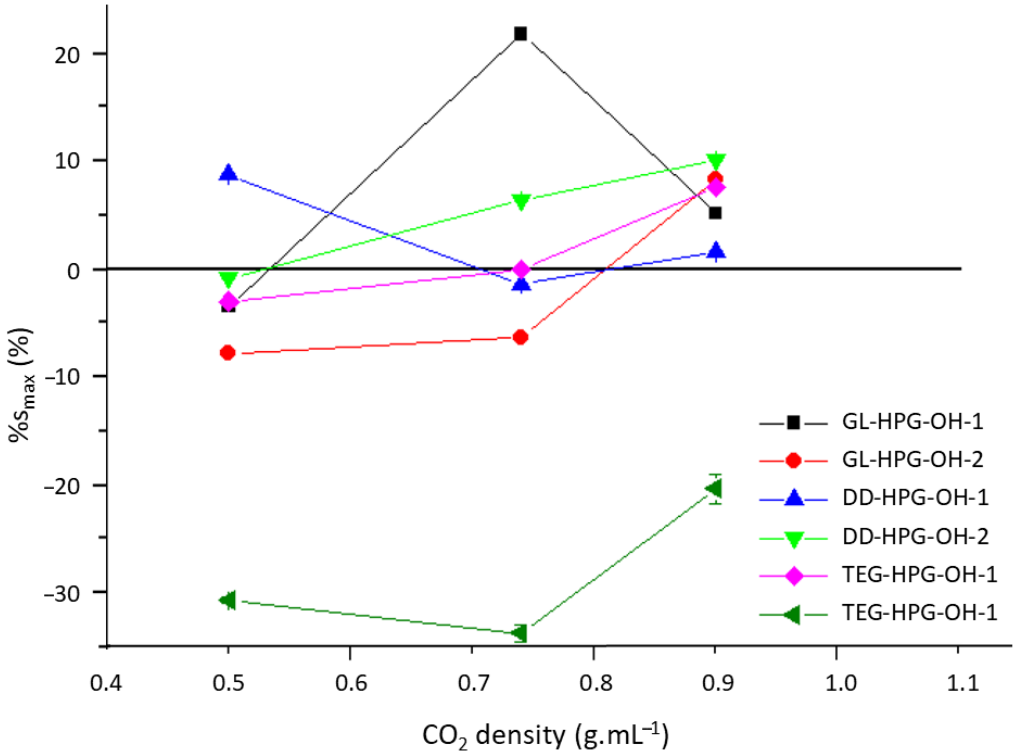

Figure 4. Final expansion of the HPG-OHs in function of the density of the system.

It is observed that the %s are small for all polymers and even negative in some conditions. The solubilization of CO_2 in a polymeric matrix depends on the intermolecular interactions between the polymer chains and between the polymer and solvent, and on the free volume of the polymer [17,27–29]. In these systems, the intermolecular interaction between polymer and solvent is weak due to the absence of specific interactions; moreover, the interaction polymer–polymer is strong due to the presence of hydrogen bonds, resulting in low solubilities of CO_2 into the polymers, caused mainly by its penetration in the free volume of the polymeric phase. Indeed, branched polymers present higher free volumes when compared to their linear analogs due to the natural space between the branches and to the difficulty in packing the chains due to their irregular form. It is possible to propose that this solubilization can generate three conditions that influence the expansion: (i) The separation of the polymer chains after the penetration of CO_2 into the free volume regions, causing the decrease in viscosity and contributing to volume expansion; (ii) the retraction of the polar groups of the polymer chains due to the decrease in the polarity of the system, which is especially important for the polymers bearing more hydroxyl groups per volume, i.e., the HPG-OH with lower Mn, contributing to a decrease in the volume of the polymer phase; and (iii) the reorganization of the chains due to the increase in their freedom (mobility) caused by (i), which can lead to their organization and compaction, contributing to a decrease in the volume of the polymer phase. Indeed, CO_2 is known for

acting as a plasticizer in polymer matrices [30,31] and by its ability to allow the organization of polymer chains. It is able, for instance, to increase the crystallinity of semi-crystalline polymers [32,33]. The absence of specific interactions between the polymer and solvent and, therefore, efficient solvation, is the basis to understand the low solubility of CO_2 into the polymer phase and the low efficiency of (i) in promoting an increase in expansion.

It is expected that the polymers bearing the core DD, with lower polarity and lower interaction among their chains, present higher solubilization of CO_2, and that more polar polymers would present a lower solubilization of CO_2. Indeed, it was observed that DD-HPG-OH polymers presented a higher expansion than TEG-HPG-OH polymers due to higher CO_2 solubility in the former. However, their expansions were lower than those for the GL-HPG-OH polymers due to their better capacity for organization and compaction, caused by their lower DB. In general, the expansion increases with the increase in the density of the system, due to the increase in the solvent power of CO_2. However, this trend was not observed for the polymer GL-HPG-OH-1, showing that the rearrangement of the chains and the retraction of the hydroxyl groups are potentialized for this polymer.

3.4. Behavior in Dense CO_2 of the HPG-Acs

The study of the expansion of HPG-Acs was performed using the same conditions used for HPG-OHs: 0.50 g.mL^{-1} {10 MPa, 45 °C}, 0.74 g.mL^{-1} {15 MPa, 45 °C}, and 0.90 g.mL^{-1} {25 MPa, 35 °C}. The kinetic of expansion was followed and is presented in the supporting information. During preliminary expansion experiments, the polymer DD-HPG-Ac-1 presented a complete solubilization in the $scCO_2$ phase and, because of this, it was studied using only the cloud point experiment instead.

The HPG-Acs along time, presented an increase in expansion that reached a maximum value ($\%s_{max}$) before decreasing and stabilizing ($\%s_{final}$). The time needed for the polymers to reach the $\%s_{max}$ was reported as $t_{\%s\ max}$. Moreover, the weight loss (%) of the samples, referring to the solubilized mass, was determined. The results of the expansion experiment are presented in Table 4.

Table 4. Expansion results for the HPG-Acs.

Polymer	Condition	$\%s_{max}$ (%)	$\%s_{final}$ (%)	$t_{\%s\ max}$ (min)	Weight Loss (%)
GL-HPG-Ac-1	0.50 g.mL^{-1}, 10 MPa, 45 °C	41	40	22	6.7
	0.74 g.mL^{-1}, 15 MPa, 45 °C	66	61	67	9.8
	0.90 g.mL^{-1}, 25 MPa, 35 °C	57	53	66	15.0
GL-HPG-Ac-2	0.50 g.mL^{-1}, 10 MPa, 45 °C	23	23	21	1.8
	0.74 g.mL^{-1}, 15 MPa, 45 °C	29	28	65	9.1
	0.90 g.mL^{-1}, 25 MPa, 35 °C	56	50	96	25.1
DD-HPG-Ac-2	0.50 g.mL^{-1}, 10 MPa, 45 °C	59	58	61	6.1
	0.74 g.mL^{-1}, 15 MPa, 45 °C	57	54	43	12.0
	0.90 g.mL^{-1}, 25 MPa, 35 °C	1	−7	10	37.8
TEG-HPG-Ac-1	0.50 g.mL^{-1}, 10 MPa, 45 °C	33	33	88	6.5
	0.74 g.mL^{-1}, 15 MPa, 45 °C	36	35	60	7.9
	0.90 g.mL^{-1}, 25 MPa, 35 °C	41	28	65	21.2
TEG-HPG-Ac-2	0.50 g.mL^{-1}, 10 MPa, 45 °C	45	44	47	−0.6
	0.74 g.mL^{-1}, 15 MPa, 45 °C	38	38	77	4.7
	0.90 g.mL^{-1}, 25 MPa, 35 °C	48	48	91	10.3

The variation in the volume of the polymers along time (Table 4, third and fourth column) can be attributed to three processes that occur simultaneously: (i) A significant

solubilization of CO_2 into the polymeric phase, which increases the volume of this phase, (ii) the partial solubilization of the polymers in $scCO_2$, which contributes to the decrease in the volume of the polymer phase, and (iii) the rearrangement of the polymer chains, which contributes to the decrease in the volume of the polymer phase. It is also important to note that because of the dispersity (Đ) of these polymers, the lower Mn chains will have higher solubilities in $scCO_2$ than the higher Mn ones. After the polymer phase reaches the $\%s_{max}$, process (ii) becomes more significant than (i), which explains the decrease in the observed %s. Process (iii) could not be clearly evaluated due to the predominant contributions of processes (i) and (ii).

When the values of the %s for the HPG-Acs (and the solubilization of DD-HPG-Ac-1 in $scCO_2$) are compared with the values of %s for the HPG-OHs, it is evident that acetylation played a significant role in increasing CO_2 solubility by increasing its interaction with the polymers. Firstly, by reducing the interaction of polymer–polymer through the elimination of the hydrogen bonds of their hydroxyl groups, as evidenced by the DSC analysis. Secondly, by creating specific Lewis's acid–base interactions between polymer and CO_2 [5]. Indeed, the acetyl group is recognized as a group that promotes CO_2-philicity, therefore promoting the solubility of materials in CO_2 and the solubility of CO_2 into a phase of the material [7,34,35]. The acetylation decreases the polarity of the polymers, but their order of polarity remains the same as for the HPG-OHs (except for the polymers TEG-HPG-Ac-1 and TEG-HPG-Ac-2, which have similar polarities since their Mn became alike after acetylation). Higher polarities represent stronger polymer–polymer interactions and, therefore, lower CO_2-philicities.

Figure 5 shows the $\%s_{max}$ of HPG-Acs for the different densities tested. The $\%s_{max}$ reached up to 66% and, in general, increases with the increase in the density of CO_2 and the decrease in their polarities and Mns. However, as the expansion of the polymer phase occurs simultaneously with its solubilization, the weight loss of the samples needs to be evaluated together with the $\%s_{max}$. This allows us to have a better understanding of the system and of the samples that do not follow that tendency. For instance, the less polar polymers, DD-HPG-Ac-2 and GL-HPG-Ac-1, present a decrease in their $\%s_{max}$ for higher CO_2 densities, which is in agreement with their higher weight loss under these conditions. Indeed, preliminary tests (Supplementary Materials, Figures S68 and S69) showed partial solubility for HPG-Acs, evidenced by their cloud points. As observed for the expansion experiment, the polymers presented higher weight losses for lower polarities, and the condition of the higher weight loss was the one of higher density {0.90 $g.mL^{-1}$, 25 MPa, 35 °C}, because, when increasing density, the solubilizing capacity of the sc-CO_2 increases.

The time needed for the polymers to reach $\%s_{max}$ decreases as their CO_2-philicities increase, evidencing that a greater interaction of CO_2 with the polymer phase leads to faster processes. Wind et al. showed the kinetics of swelling of polyimides and also attributed faster swelling to a greater suitability to CO_2 absorption [36].

Figure 6 shows the phase diagram obtained for DD-HPG-Ac-1 for the cloud point experiment. It is shown that the cloud points present higher values of pressure as the temperature increases, ranging from to 4.3 MPa at 25 °C to 13.5 MPa at 65 °C. This occurs because at higher temperatures, higher pressures are needed to generate densities that allow for enough solvation for the solubilization of the polymer. Indeed, Fortunatti-Montoya et al. showed that an increase in pressure from ca. 9.4 to 11.4 MPa is needed to solubilize 56 mg of triacetyl glycerol (the lowest Mw analog of our studied polymers) in 1 g of $scCO_2$ when the temperature increased from 42 °C to 50 °C [37]; Gregorowicz et al. studied a higher Mw acetylated hyperbranched polyglycerol and showed that the cloud points present an increase in pressure from around 70 to 110 MPa when the temperature increases from around 32 °C to 152 °C [38]. The cloud points presented in this work for different

concentrations have similar values for the same experimental conditions, showing that precipitation is efficient at the cloud point.

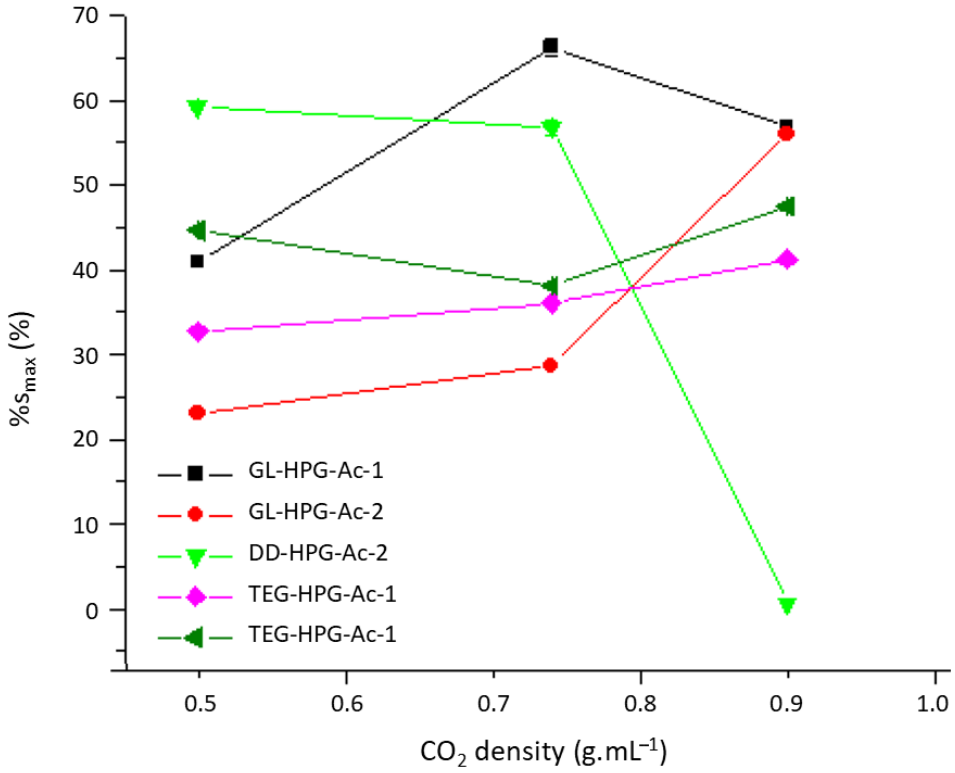

Figure 5. Maximum expansion of the HPG-Acs as a function of the density of the system.

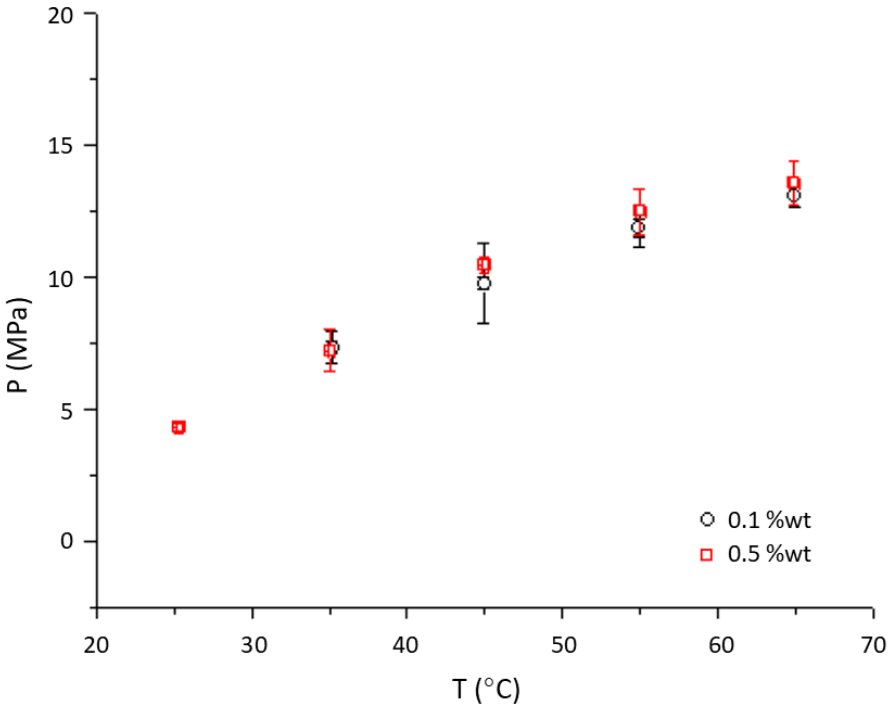

Figure 6. Phase diagram of the polymer DD-HPG-Ac-1.

4. Conclusions

The acetylation of hyperbranched polyglycerols was shown to be an efficient way to increase their CO_2-philicity for all the polymers studied. This increase was reflected

in the increase in both polymer expansion and polymer solubility in $scCO_2$ media. The expansion of the acetylated polymers reached up to 66% of their initial volume, while for non-acetylated ones, in general, the expansion did not exceed 10% and was negative in some conditions due to the plasticizing effect of CO_2, which allowed for the accommodation of the polymer chains. All acetylated polymers presented solubility in $scCO_2$; it was complete for the polymer bearing a dodecanediol core and lower Mn, and only partial for the others. Indeed, not only acetylation, but also the structure of the polymers, were relevant for their interaction with CO_2. The use of polar and apolar cores and different Mns allowed for the evaluation of polymers with different polarities, and it was shown that decreasing their polarities lead to lower polymer–polymer interactions, which contributed to higher CO_2-philicities and, therefore, a higher expansion/solubilization in $scCO_2$. Therefore, the characterization of the behavior of those polymers in $scCO_2$ evidenced relevant structural characteristics that contributed to the solubilization of the CO_2 into the polymer phase and the solubilization of the polymers in the CO_2 phase, as well as the role of the density of the system on these processes. Indeed, increasing the density of the system caused an increase in the expansion/solubilization of the acetylated polymers.

HPG-Acs are therefore potential materials for biphasic (polymer/CO_2) reaction systems in processes using CO_2 either as a solvent or as a reactant, and in temperatures up to at least 200 °C, where good absorption of CO_2 into the second phase of the system is required, such as catalyzed chemical reactions. The data presented gives a basis to understand the role of process conditions and to select or design an HPG-Ac that would best fit a given process as a reaction media, support for catalysts, or even co-solvent or phase transfer agent.

Supplementary Materials: The following supporting information can be downloaded at: https://www.mdpi.com/article/10.3390/pr13082510/s1, Equation (S1). Calculation of the average number of mols of hydroxyl groups per mol of HPG-OH; Figure S1. Determination of the heights of the polymer in different experimental conditions; Table S1. Calibration data for the determination of the volume of the polymer in the volumetric expansion experiment; Figure S2. Kinetic expansion of the polymer GL-HPG-OH-1; Figure S3. Kinetic expansion of the polymer GL-HPG-OH-2; Figure S4. Kinetic expansion of the polymer DD-HPG-OH-1; Figure S5. Kinetic expansion of the polymer DD-HPG-OH-2; Figure S6. Kinetic expansion of the polymer TEG-HPG-OH-1; Figure S7. Kinetic expansion of the polymer TEG-HPG-OH-2; Figure S8. Kinetic expansion of the polymer GL-HPG-Ac-1; Figure S9. Kinetic expansion of the polymer GL-HPG-Ac-2; Figure S10. Kinetic expansion of the polymer DD-HPG-Ac-2; Figure S11. Kinetic expansion of the polymer TEG-HPG-Ac-1; Figure S12. Kinetic expansion of the polymer TEG-HPG-Ac-2; Figure S13. ESI-TOF-MS spectrum of polymer GL-HPG-OH-1; Figure S14. ESI-TOF-MS spectrum of polymer GL-HPG-OH-2; Figure S15. ESI-TOF-MS spectrum of polymer DD-HPG-OH-1; Figure S16. ESI-TOF-MS spectrum of polymer DD-HPG-OH-2; Figure S17. ESI-TOF-MS spectrum of polymer TEG-HPG-OH-1; Figure S18. ESI-TOF-MS spectrum of polymer TEG-HPG-OH-2; Figure S19. ^{1}H NMR spectrum of polymer GL-HPG-OH-1; Figure S20. ^{13}C NMR spectrum of polymer GL-HPG-OH-1; Figure S21. ^{1}H NMR spectrum of polymer GL-HPG-OH-2; Figure S22. ^{13}C NMR spectrum of polymer GL-HPG-OH-2; Figure S23. ^{1}H NMR spectrum of polymer DD-HPG-OH-1; Figure S24. ^{13}C NMR spectrum of polymer DD-HPG-OH-1; Figure S25. ^{1}H NMR spectrum of polymer DD-HPG-OH-2; Figure S26. ^{13}C NMR spectrum of polymer DD-HPG-OH-2; Figure S27. ^{1}H NMR spectrum of polymer TEG-HPG-OH-1; Figure S28. ^{13}C NMR spectrum of polymer TEG-HPG-OH-1; Figure S29. ^{1}H NMR spectrum of polymer TEG-HPG-OH-2; Figure S30. ^{13}C NMR spectrum of polymer TEG-HPG-OH-2; Figure S31. TGA thermogram of polymer GL-HPG-OH-1; Figure S32. TGA thermogram of polymer GL-HPG-OH-2; Figure S33. TGA thermogram of polymer DD-HPG-OH-1; Figure S34. TGA thermogram of polymer DD-HPG-OH-2; Figure S35. TGA thermogram of polymer TEG-HPG-OH-1; Figure S36. TGA thermogram of polymer TEG-HPG-OH-2; Figure S37. DSC thermograms of the polymers: black lines (GL-HPG-OH-1), blue lines (GL-HPG-OH-2), green lines (DD-HPG-OH-1), red lines (DD-HPG-OH-2), pink lines (TEG-

HPG-OH-1) and violet lines (TEG-HPG-OH-2). Solid lines refer to the DSC curves and dashed lines refers to their derivate curves; Figure S38. ESI-TOF-MS spectrum of polymer GL-HPG-Ac-1; Figure S39. ESI-TOF-MS spectrum of polymer GL-HPG-Ac-2; Figure S40. ESI-TOF-MS spectrum of polymer DD-HPG-Ac-1; Figure S41. ESI-TOF-MS spectrum of polymer DD-HPG-Ac-2; Figure S42. ESI-TOF-MS spectrum of polymer TEG-HPG-Ac-1; Figure S43. ESI-TOF-MS spectrum of polymer TEG-HPG-Ac-2; Figure S44. ^{1}H NMR spectrum of polymer GL-HPG-Ac-1; Figure S45. ^{13}C NMR spectrum of polymer GL-HPG-Ac-1; Figure S46. ^{1}H NMR spectrum of polymer GL-HPG-Ac-2; Figure S47. ^{13}C NMR spectrum of polymer GL-HPG-Ac-2; Figure S48. ^{1}H NMR spectrum of polymer DD-HPG-Ac-1; Figure S49. ^{13}C NMR spectrum of polymer DD-HPG-Ac-1; Figure S50. ^{1}H NMR spectrum of polymer DD-HPG-Ac-2; Figure S51. ^{13}C NMR spectrum of polymer DD-HPG-Ac-2; Figure S52. ^{1}H NMR spectrum of polymer TEG-HPG-Ac-1; Figure S53. ^{13}C NMR spectrum of polymer TEG-HPG-Ac-1; Figure S54. ^{1}H NMR spectrum of polymer TEG-HPG-Ac-2; Figure S55. ^{13}C NMR spectrum of polymer TEG-HPG-Ac-2; Figure S56. TGA thermogram of polymer GL-HPG-Ac-1; Figure S57. TGA thermogram of polymer GL-HPG-Ac-2; Figure S58. TGA thermogram of polymer DD-HPG-Ac-1; Figure S59. TGA thermogram of polymer DD-HPG-Ac-2; Figure S60. TGA thermogram of polymer TEG-HPG-Ac-1; Figure S61. TGA thermogram of polymer TEG-HPG-Ac-2; Figure S62. DSC thermograms of the polymer GL-HPG-Ac-1; Figure S63. DSC thermograms of the polymer GL-HPG-Ac-2; Figure S64. DSC thermograms of the polymer DD-HPG-Ac-1; Figure S65. DSC thermograms of the polymer DD-HPG-Ac-2; Figure S66. DSC thermograms of the polymer TEG-HPG-Ac-1; Figure S67. DSC thermograms of the polymer TEG-HPG-Ac-2; Figure S68. Clouds points of a partially solubilized DD-HPG-Ac; Figure S69. Clouds points of a partially solubilized TEG-HPG-Ac.

Author Contributions: Conceptualization, R.C.B. and L.P.M.-O.; methodology, R.C.B. and L.P.M.-O.; validation, R.C.B. and L.P.M.-O.; formal analysis, L.P.M.-O.; investigation, L.P.M.-O.; resources, R.C.B.; data curation, L.P.M.-O.; writing—original draft preparation, L.P.M.-O.; writing—review and editing, L.P.M.-O. and R.C.B.; visualization, L.P.M.-O.; supervision, R.C.B.; project administration, R.C.B. All authors have read and agreed to the published version of the manuscript.

Funding: This work was supported by the Brazilian National Council for Scientific and Technological Development/CNPq (140719/2010-5, 200869/2024-8); the Research Foundation of the State of São Paulo/FAPESP (05/59396-4, 2011/20168-8, 2020/15230-5); the Coordination of Improvement of Higher Education Personnel/CAPES; the National Institute of Science and Technology of Environmental Studies/INCT. We gratefully acknowledge the support of the RCGI – Research Centre for Greenhouse Gas Innovation (23.1.8493.1.9), hosted by the University of São Paulo (USP) and sponsored by FAPESP – São Paulo Research Foundation (2020/15230-5) and sponsors (specially SHELL), as well as the strategic importance of the support given by ANP (Brazil's National Oil, Natural Gas and Biofuels Agency) through the R&DI levy regulation.

Data Availability Statement: The data presented in this study are available in "Effect of Acetylation on the Behavior of Hyperbranched Polyglycerols in Supercritical CO_2" and its Supplementary Information Material.

Acknowledgments: The authors acknowledge the Brazilian National Research Council (CNPq), the Research Foundation of the State of São Paulo (FAPESP), the Coordination of Improvement of Higher Education Personnel (CAPES), and the INCT (National Institute of Science and Technology) of Environmental Studies and the Research Centre for Greenhouse Gas Innovation (RCGI)/Shell for the financial support.

Conflicts of Interest: The authors declare no conflicts of interest.

References

1. Kim, Y.H.; Webster, O.W. Hyperbranched Polyphenylenes. *Macromolecules* **1992**, *25*, 5561–5572. [CrossRef]
2. Paleos, C.M.; Tsiourvas, D.; Sideratou, Z. Molecular engineering of dendritic polymers and their application as drug and gene delivery systems. *Mol. Pharm.* **2007**, *4*, 169–188. [CrossRef]

3. Wiltshire, J.T.; Qiao, G.G. Recent Advances in Star Polymer Design: Degradability and the Potential for Drug Delivery. *Aust. J. Chem.* **2007**, *60*, 699–705. [CrossRef]
4. Liu, H.; Jiang, A.; Guo, J.; Uhrich, K.E. Unimolecular Micelles: Synthesis and Characterization of Amphiphilic Polymer Systems. *J. Polym. Sci. Part A Polym. Chem.* **1999**, *37*, 703–711. [CrossRef]
5. Raveendran, P.; Ikushima, Y.; Wallen, S.L. Polar Attributes of Supercritical Carbon Dioxide. *Acc. Chem. Res.* **2005**, *38*, 478–485. [CrossRef]
6. Kerton, F.M. *Alternative Solvents for Green Chemistry*; Royal Society of Chemistry: Cambridge, UK, 2009.
7. Nasir, M.I.; Bernards, M.A.; Charpentier, P.A. Acetylation of soybean lecithin and identification of components for solubility in supercritical carbon dioxide. *J. Agric. Food Chem.* **2007**, *55*, 1961–1969. [CrossRef] [PubMed]
8. Potluri, V.K.; Hamilton, A.D.; Karanikas, C.F.; Bane, S.E.; Xu, J.; Beckman, E.J.; Enick, R.M. The high CO_2-solubility of peracetylated α-, β-, and γ-cyclodextrin. *Fluid Phase Equilibria* **2003**, *211*, 211–217. [CrossRef]
9. Lambert, A.; Ingrosso, F. A Molecular Dynamics Study of the Solvation Properties of Sugars in Supercritical Carbon Dioxide. *Molecules* **2025**, *30*, 1256. [CrossRef]
10. Huang, W.-A.; Su, R.; Wang, J.-W.; Fan, Y.; Jiang, L.; Li, X.; Cao, J. Synthesis and characterization of a host–guest complex based on acetylated-β-cyclodextrin and its application in improving the viscosity of supercritical carbon dioxide. *Fuel* **2024**, *363*, 130837. [CrossRef]
11. Maia-Obi, L.P.; Vidinha, P.; Ferraz, H.G.; Bazito, R.C. Non-Inclusion Complexation of Peracetylated β-Cyclodextrin with Ibuprofen in Supercritical Carbon Dioxide. *J. Supercrit. Fluids* **2021**, *169*, 105098. [CrossRef]
12. Rindfleisch, F.; DiNoia, T.P.; McHugh, M.A. Solubility of polymers and copolymers in supercritical CO_2. *J. Phys. Chem.* **1996**, *100*, 15581–15587. [CrossRef]
13. Sato, Y.; Takikawa, T.; Takishima, S.; Masuoka, H. Solubilities and diffusion coefficients of carbon dioxide in poly(vinyl acetate) and polystyrene. *J. Supercrit. Fluids* **2001**, *19*, 187–198. [CrossRef]
14. Zhang, S.; Chen, K.; Liang, L.; Tan, B. Synthesis of oligomer vinyl acetate with different topologies by RAFT/MADIX method and their phase behaviour in supercritical carbon dioxide. *Polymer* **2013**, *54*, 5303–5309. [CrossRef]
15. Gong, H.; Gui, W.; Zhang, H.; Lv, W.; Xu, L.; Li, Y.; Dong, M. Molecular dynamics study on the dissolution behaviors of poly(vinyl acetate)-polyether block copolymers in supercritical CO_2. *J. Appl. Polym. Sci.* **2020**, *138*, 50151. [CrossRef]
16. Valor, D.; Montes, A.; Cózar, A.; Pereyra, C.; de la Ossa, E.M. Development of Porous Polyvinyl Acetate/Polypyrrole/Gallic Acid Scaffolds Using Supercritical CO_2 as Tissue Regenerative Agents. *Polymers* **2022**, *14*, 672. [CrossRef]
17. Champeau, M.; Thomassin, J.-M.; Tassaing, T.; Jérôme, C. Drug loading of polymer implants by supercritical CO_2 assisted impregnation: A review. *J. Control. Release* **2015**, *209*, 248–259. [CrossRef]
18. Medina-Gonzalez, Y.; Camy, S.; Condoret, J.-S. $ScCO_2$/green solvents: Biphasic promising systems for cleaner chemicals manufacturing. *ACS Sustain. Chem. Eng.* **2014**, *2*, 2623–2636. [CrossRef]
19. Sunder, A.; Hanselmann, R.; Frey, H.; Mülhaupt, R. Controlled Synthesis of Hyperbranched Polyglycerols by Ring-Opening Multibranching Polymerization. *Macromolecules* **1999**, *32*, 4240–4246. [CrossRef]
20. Wu, W.B.; Chiu, W.Y.; Liau, W.B. Casting solvent effect on crystallization behavior of poly(vinyl acetate)/poly(ethylene oxide) blends: DSC study. *J. Appl. Polym. Sci.* **1997**, *64*, 411–421. [CrossRef]
21. Rasband, W. ImageJ. Available online: http://imagej.nih.gov/ij/ (accessed on 15 July 2025).
22. Xu, Y.; Gao, C.; Kong, H.; Yan, D.; Luo, P.; Li, W.; Mai, Y. One-pot synthesis of amphiphilic core-shell suprabranched macromolecules. *Macromolecules* **2004**, *37*, 6264–6267. [CrossRef]
23. Samuel, H.S.; Nweke, M.U.; Etim, E.E. Supercritical Fluids: Properties, Formation and Applications. *J. Eng. Ind. Res.* **2023**, *4*, 176–188. [CrossRef]
24. Goodwin, A.; Baskaran, D. Inimer Mediated Synthesis of Hyperbranched Polyglycerol via Self-Condensing Ring-Opening Polymerization. *Macromolecules* **2012**, *45*, 9657–9665. [CrossRef]
25. Rokicki, G.; Rakoczy, P.; Parzuchowski, P.; Sobiecki, M. Hyperbranched aliphatic polyethers obtained from environmentally benign monomer: Glycerol carbonate. *Green Chem.* **2005**, *7*, 529–539. [CrossRef]
26. Frey, H.; Haag, R. Dendritic polyglycerol: A new versatile biocompatible material. *Rev. Mol. Biotechnol.* **2002**, *90*, 257–267. [CrossRef]
27. Upton, C.E.; Kelly, C.A.; Shakesheff, K.M.; Howdle, S.M. One dose or two? The use of polymers in drug delivery. *Polym. Int.* **2007**, *56*, 1457–1460. [CrossRef]
28. Pini, R.; Storti, G.; Mazzotti, M.; Tai, H.; Shakesheff, K.M.; Howdle, S.M. Howdle, Sorption and swelling of poly(DL-lactic acid) and poly(lactic-co-glycolic acid) in supercritical CO_2: An experimental and modeling study. *J. Polym. Sci. B Polym. Phys.* **2008**, *46*, 483–496. [CrossRef]
29. Yoda, S.; Sato, K.; Oyama, H.T. Impregnation of paclitaxel into poly(dl-lactic acid) using high pressure mixture of ethanol and carbon dioxide. *RSC Adv.* **2011**, *1*, 156–162. [CrossRef]

30. Alessi, P.; Cortesi, A.; Kikic, I.; Vecchione, F. Plasticization of polymers with supercritical carbon dioxide: Experimental determination of glass-transition temperatures. *J. Appl. Polym. Sci.* **2003**, *88*, 2189–2193. [CrossRef]
31. Kazarian, S.G.; Vincent, M.F.; Bright, F.V.; Liotta, C.L.; Eckert, C.A. Specific Intermolecular Interaction of Carbon Dioxide with Polymers. *J. Am. Chem. Soc.* **1996**, *118*, 1729–1736. [CrossRef]
32. Zhai, W.; Ko, Y.; Zhu, W.; Wong, A.; Park, C.B. A Study of the Crystallization, Melting, and Foaming Behaviors of Polylactic Acid in Compressed CO_2. *Int. J. Mol. Sci.* **2009**, *10*, 5381–5397. [CrossRef]
33. Lei, Z.; Ohyabu, H.; Sato, Y.; Inomata, H.; Smith, R.L. Solubility, swelling degree and crystallinity of carbon dioxide–polypropylene system. *J. Supercrit. Fluids* **2007**, *40*, 452–461. [CrossRef]
34. Shen, Z.; McHugh, M.; Xu, J.; Belardi, J.; Kilic, S.; Mesiano, A.; Bane, S.; Karnikas, C.; Beckman, E.; Enick, R. CO_2-solubility of oligomers and polymers that contain the carbonyl group. *Polymer* **2003**, *44*, 1491–1498. [CrossRef]
35. Sarbu, T.; Styranec, T.J.; Beckman, E.J. Design and synthesis of low cost, sustainable CO_2-philes. *Ind. Eng. Chem. Res.* **2000**, *39*, 4678–4683. [CrossRef]
36. Wind, J.D.; Sirard, S.M.; Paul, D.R.; Green, P.F.; Johnston, K.P.; Koros, W.J. Relaxation Dynamics of CO_2 Diffusion, Sorption, and Polymer Swelling for Plasticized Polyimide Membranes. *Macromolecules* **2003**, *36*, 6442–6448. [CrossRef]
37. Fortunatti-Montoya, M.; Sánchez, F.A.; Hegel, P.E.; Pereda, S. Fractionation of glycerol acetates with supercritical CO_2. *J. Supercrit. Fluids* **2019**, *153*, 104575. [CrossRef]
38. Gregorowicz, J.; Fraś, Z.; Parzuchowski, P.; Rokicki, G.; Kusznerczuk, M.; Dziewulski, S. Phase behaviour of hyperbranched polyesters and polyethers with modified terminal OH groups in supercritical solvents. *J. Supercrit. Fluids* **2010**, *55*, 786–796. [CrossRef]